Sci. U.S.A. 71, 4237–4240.
Kayne, M. S., and Cohn, M. (1974), *Biochemistry 13,* 4159–4165.
Kim, S. H., Quigley, G. J., Suddath, F. L., McPherson, A., Sneden, D., Kim, J. J., Weingierl, J., and Rich, A. (1973), *Science 179,* 285–288.
Kim, S. H., Sussman, J. L., Suddath, F. L., Quigley, G. J., McPherson, A., Wang, A. H. J., Seeman, N. C., and Rich, A. (1974), *Proc. Natl. Acad. Sci. U.S.A. 71,* 4970–4974.
Klug, A., Ladner, J., and Robertus, J. D. (1974), *J. Mol. Biol. 89,* 511–516.
Rialdi, G., Levy, J., and Biltonen, R. (1972), *Biochemistry 11,* 2472–2482.
Robertus, J. D., Ladner, J. E., Finch, J. T., Rodes, D., Brown, R. S., Clark, F. F. C., and Klug, A. (1974), *Nature (London) 250,* 546–551.
Sander, C., and Ts'o, P. O. P. (1971), *J. Mol. Biol. 55,* 1–21.
Schreier, A. A., and Schimmel, P. R. (1974), *J. Mol. Biol. 86,* 601–620.
Slavin, W. (1968), in Chemical Analysis 25, Atomic Absorption Spectroscopy, Elving, P. J., and Kolthoff, I. M., Ed., New York, N.Y., Interscience.
Stein, A., and Crothers, D. M. (1976), *Biochemistry,* following paper in this issue.
Wolfson, J. M., and Kearns, D. R. (1974), *J. Am. Chem. Soc. 96,* 3653–3654.
Yang, S. K., and Crothers, D. M. (1972), *Biochemistry 11,* 4375–4381.

Conformational Changes of Transfer RNA. The Role of Magnesium(II)†

A. Stein‡ and D. M. Crothers*

ABSTRACT: Magnesium ions added to $tRNA^{fMET}_1$ selectively stabilize the dihydrouridine helix–tertiary structural region. Low Mg^{2+} levels have little direct effect on the remaining three cloverleaf helices, but these are prevented from melting independently when their intrinsic T_m is surpassed by the T_m of the tertiary structure. At high Mg^{2+} concentration the thermal unfolding of $tRNA^{fMet}_1$ is approximately a two-state, concerted transition from the globular native structure to the random coil, in contrast to the sequential unfolding observed without Mg^{2+}. We interpret the kinetics of refolding to mean that the D helix serves as a required nucleus for the rate-limiting step of tertiary structure formation. We found that unfolding of the tertiary structure leads to loss of the tightly bound Mg^{2+} ions, and showed with a Mn^{2+}-sensitive fluorescent indicator that the rate of Mn^{2+} release is the same as the rate of unfolding the tertiary structure. Hence the tightly bound divalent ion must be located in a site formed by the tertiary structure–D helix region of the molecule.

Many biological macromolecules, both proteins and nucleic acids, undergo conformational changes in the course of their function. Hemoglobin when binding oxygen, and DNA while undergoing replication are well-known examples. Conformational changes must occur during the complex reactions of ribosome-mediated protein synthesis, but the mechanical events in this fundamental biological process remain obscure. One of the key components in protein synthesis is tRNA. Its biochemical role as carrier of amino acid and anticodon are well known. More hypothetical is the possibility that tRNA performs an important mechanical function in protein synthesis by undergoing major conformational changes when bound to the ribosome. There is some evidence suggesting that tRNA structure may unfold when bound to the 30S subunit (Schwarz et al., 1974; Erdman et al., 1973). Furthermore, one can see distinct mechanistic advantages in unfolding enough of the tRNA tertiary structure to allow independent motion of amino acid acceptor and anticodon portions of the molecule (Crothers, 1975).

Our current series of experiments has focused on conformational changes of purified $tRNA^{fMet}$ in solution. Some, but certainly not all, of these changes may be related to tRNA function; others need to be characterized in order to understand how newly synthesized tRNA (or its precursor) can fold up into the native structure. The molecular mechanism of thermal unfolding of $tRNA^{fMet}$ in the absence of Mg^{2+} has previously been investigated in some detail by a combination of relaxation kinetics and nuclear magnetic resonance (NMR) spectroscopy (Crothers et al., 1974). Four distinct relaxations were found and characterized, corresponding to effectively independent sequential melting of the tertiary structure–D helix region and the three remaining helical arms.

In this paper we present the effect of increasing concentrations of Mg^{2+} on these known relaxations. The influence of Mg^{2+} on the thermal stability and dynamic properties of particular regions of the molecule is elucidated, as is the molecular pathway of thermal unfolding in the presence of Mg^{2+}. We also present a mechanism for the rate-determining step in refolding the native structure, involving formation of tertiary bonds to the D helix, which serves as a re-

† From the Department of Chemistry, Yale University, New Haven, Connecticut 06520. *Received April 22, 1975.* Supported by Grants GM12589 and GM21966 from the National Institute of General Medical Science.
‡ Supported by American Cancer Society Fellowship PF-858.

quired nucleus. Our measurements permit calculation of the number of Mg^{2+} ions released on melting known parts of the molecule. We also measured directly the release of Mn^{2+} ions upon unfolding the tertiary structure. A fluorescence temperature-jump technique was used in which the tRNA melting equilibrium was coupled to a fast equilibrium between Mn^{2+} and a chelating dye (noninteracting with tRNA) which exhibits a large fluorescence decrease upon binding Mn^{2+}. Thus, the amplitude of the fluorescence relaxation signal with the characteristic relaxation time of the tertiary unfolding is a direct measure of the release of metal ions stabilizing the tertiary structure.

The general role that we find for Mg^{2+} is a marked preferential stabilization of the native tertiary structure. The tertiary interaction seems to exist in high Na^+ without Mg^{2+}, but it is the least stable part of the molecule under those conditions. Addition of Mg^{2+} makes it one of the most stable parts. Conversely, the tertiary structure provides the strong Mg^{2+} binding site, which disappears when the tertiary structure unfolds. Conformational changes of tRNA in vivo could clearly be triggered by ribosome-mediated removal or addition of Mg^{2+}.

This paper completes our current series on *Escherichia coli* $tRNA^{fMet}$ (Cole et al., 1972; Cole and Crothers, 1972; Crothers et al., 1974; Bina-Stein and Crothers, 1975; Stein and Crothers, 1976). Conformational equilibria and dynamics are probably as well understood for this tRNA as for any globular macromolecule.

Materials and Methods

(*a*) *Buffers.* The buffer used for measurements on tRNA samples in the absence of Mg^{2+} contained 0.001 *M* phosphate, 0.01 *M* sodium cacodylate, 0.001 *M* EDTA, and 0.152 *M* sodium perchlorate (pH 7.0) (total Na^+ concentration 0.166 *M*). In samples containing magnesium acetate the buffer was the same except that it contained no EDTA and the sodium perchlorate concentration was 0.154 *M*. The buffer used for samples containing manganese(II) chloride contained 0.02 *M* sodium cacodylate, 0.154 *M* sodium perchlorate, pH adjusted to 7.0 with HCl. It was found that Mn^{2+} was precipitated by phosphate.

(*b*) *Relaxation measurements* in which the absorbance was monitored were performed as described previously (Cole and Crothers, 1972). The temperature jump size was 1.88°C.

Our temperature-jump instrument was modified for fluorescence detection at a right angle to the incident beam using the same detector system. The signal to noise ratio was satisfactory for measuring relaxation processes in the msec range. A 3-ml fluorescence temperature-jump cell from Messanlagen (Göttingen) was used.

The fluorescence temperature-jump instrument was used to measure directly the divalent ions released upon melting the tertiary and D helix interactions of $tRNA^{fMet}_1$ by coupling the tRNA melting equilibrium to the equilibrium between the metal ions and a chelating fluorescent indicator dye—the bound dye being nonfluorescent. One of the few dye-metal systems found to possess the properties necessary for this experiment was the calcein blue-Mn^{2+} system. The most essential properties are: (1) a fast relaxation time for Mn^{2+}-calcein blue complexation; (2) a large optical change, produced at pH 7; (3) a dye noninteracting with tRNA. Baker-grade calcein blue was used without further purification. Its properties have been partially characterized (Diehl, 1964). Mn^{2+} has been shown to be quite similar to Mg^{2+} in its interaction with tRNA (Yarus and Rashbaum, 1972).

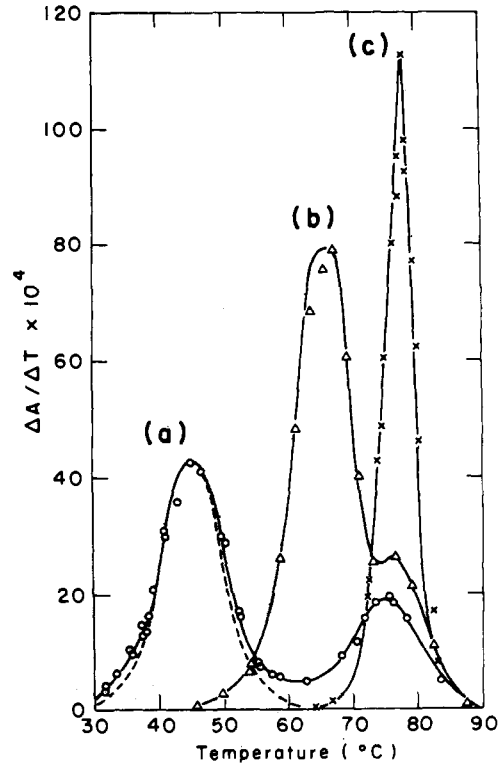

FIGURE 1: Differential thermal transition profiles for $tRNA^{fMet}_1$ temperature-jump relaxations at three Mg^{2+} concentrations. ΔA is the amplitude in absorbance units at 266 nm for the tertiary D helix, τ_2 (lower temperature), and acceptor stem, τ_5, relaxations. $\Delta A/\Delta T$ is plotted vs. the temperature corresponding to the midpoint of the temperature-jump size ΔT. (a) No Mg^{2+}, the broken curve is calculated as described in the text; (b) 0.50 m*M* Mg^{2+}; (c) 3.0 m*M* Mg^{2+}, only a single relaxation, τ_2, is observed.

The sensitivity of the dye was determined to be 36 $mV/\mu M$ change in the total Mn^{2+} concentration by titration directly in the temperature-jump cell under the same conditions and optics as used in the experiment (except that the Mn^{2+} solutions prepared did not contain tRNA). The association constant for calcein blue and Mn^{2+} at 50°C was determined to be 1.0×10^6 by titration of dilute dye solutions (absorbance of 0.13) using a null balance fluorescence spectrophotometer. An excellent fit to this titration curve could be obtained by assuming that the dye is 93% pure by weight (not dried) and that only one Mn^{2+} binds per dye molecule. The buffer solutions in the temperature-jump experiment contained 10.0 A_{260} units/ml of $tRNA^{fMet}_1$, 4.38×10^{-4} *M* dye (absorbance in the T-jump cell of 2.84 at 368 nm, the excitation wavelength), and 4.10×10^{-4} *M* total Mn^{2+}. The results of controls were as follows: (1) only a small "instantaneous" (with respect to a sweep rate of 5.0 msec/cm) signal was observed in the absence of tRNA; (2) with tRNA at the T_m of the tertiary-D helix melting, but with no Mn^{2+}, a small "instantaneous" relaxation signal was observed identical with that in the absence of both Mn^{2+} and tRNA.

Results

(*a*) *High Resolution Differential Melting Curves.* Figure 1 shows the temperature variation of the amplitude of the optical change associated with two particular relaxations at several Mg^{2+} concentrations. In the absence of Mg^{2+} the

Table I: Thermodynamic and Mg^{2+} Binding Parameters for $tRNA^{fMet}$.

Concn Mg^{2+} (M)[a]	T_m (°C)[b]	ΔH (kcal/mol)[c]	r[d]	r_s[e]	Δr[f]	X + Y[g]
0	45.2	61.2	0	0	0	D
3.4×10^{-6}	47.5	62.0	0.13	0.09		D
3.0×10^{-5}	51.0	62.3	0.79	0.47	0.48	D
1.0×10^{-4}	53.0	62.5	1.8	0.75		D
2.5×10^{-4}	59.8	72.2	3.2	0.88	2.4	D + ψ
5.0×10^{-4}	66.0	79.3	5.4	0.94	2.5	D + ψ
1.0×10^{-3}	70.4	105	8.6	0.97	3.3	D + ψ ± A
3.0×10^{-3}	78.0	≥166	15.4	0.99	≥5	D + ψ + A ± S

[a] Free Mg^{2+} concentration, established by dialysis against Mg^{2+}-containing buffer. [b] T_m defined as the maximum of the differential melting curve for the transition described by τ_2. [c] Enthalpy measured from the half-width of the differential melting curve (Crothers et al., 1974). [d] Total Mg^{2+} binding per tRNA at 4°C (Stein and Crothers, 1976). [e] Calculated Mg^{2+} binding in the strong binding site at 4°C (Stein and Crothers, 1976). [f] Mg^{2+} ion release in the transition τ_2, calculated from eq 5. [g] Regions X + Y that melt with the tertiary structure in the transition τ_2; see eq 3 and 4. D, D helix; ψ, TψC helix; A, anticodon helix; S, acceptor stem helix.

low temperature peak τ_2 (6.5 msec at T_m, the maximum) corresponds to the melting of the tertiary and D helix interactions and the high temperature peak τ_5 (1.1 msec at T_m) to the acceptor stem melting (Crothers et al., 1974). The microsecond relaxation amplitudes τ_3 and τ_4 corresponding to the melting of the TψC and anticodon arms at 61 and 70°, respectively (Crothers et al., 1974), are not shown. As the Mg^{2+} concentration is increased, the amplitude τ_2 shifts to higher temperature, increases in height and area (hyperchromicity), and narrows (corresponding to an increase in enthalpy for the process). The relaxation time gradually decreases to 2.0 msec. Note that the stem melting τ_5 is not affected until it has been "overlapped" by τ_2. The microsecond relaxations τ_3 and τ_4 (not shown) behave essentially as the stem τ_5 and no longer appear once the slow relaxation τ_2 is shifted past the T_m's of τ_3 and τ_4 in the absence of Mg^{2+}. Enthalpy and T_m values for the transition τ_2 are collected in Table I.

The observed behavior arises because stabilization of the tertiary structure prevents melting of other parts of the molecule, such as the anticodon or TψC helices. In high Mg^{2+} concentrations, all parts of $tRNA^{fMet}$ melt nearly simultaneously, approximately by a two-state or all-or-none mechanism. This is in sharp contrast to the sequential melting observed at low Mg^{2+} concentrations. The enthalpy and hyperchromicity of τ_2 increases at high Mg^{2+} because under those conditions τ_2 accounts for concerted melting of most of the molecule. This coupling between melting steps is considered more extensively in the next section.

(*b*) *Influence of Coupling on Relaxation Properties.* Relaxation amplitudes and times strictly correspond to a particular melting process (i.e., the tertiary unfolding or melting of a helical arm) only if the transitions do not signifcantly overlap on the temperature axis and are not constrained by a particular mechanism, irrespective of their separation on the time scale. In general for the unimolecular reactions considered here the relaxation times are functions of all the rate constants in the melting mechanism, and the amplitudes are functions of the enthalpy ΔH and equilibrium constant for all the reaction steps as well as the rate constants.

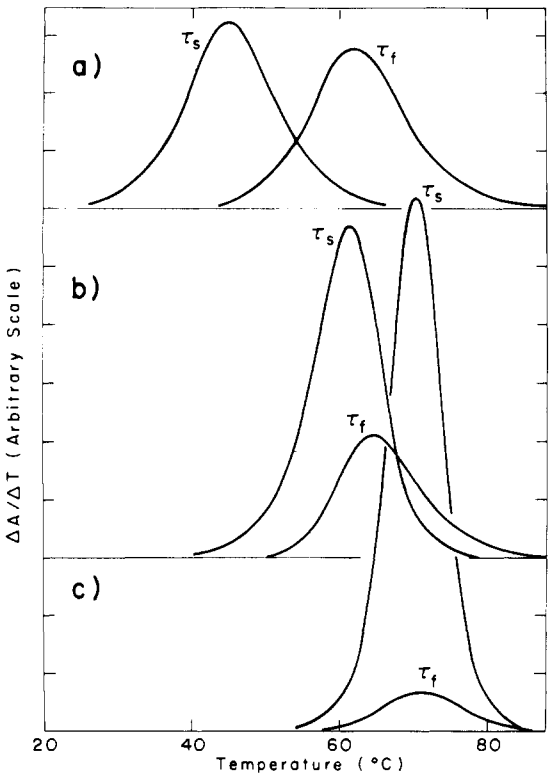

FIGURE 2: Computer simulated relaxation *amplitudes* as a function of temperature for the mechanism

$$A \overset{\text{slow}}{\rightleftharpoons} B \overset{\text{fast}}{\rightleftharpoons} C$$

to illustrate coupling effects. $T_{m_{AB}}$ is varied while other parameters remain unchanged. (a) $T_{m_{AB}} < T_{m_{BC}}$, the relaxations are effectively independent; (b) $T_{m_{AB}} = T_{m_{BC}}$, coupling occurs; (c) $T_{m_{AB}} > T_{m_{BC}}$, the relaxations are strongly coupled.

The rate equations for a particular mechanism may be written in terms of the independent concentration displacements from equilibrium X_i:

$$\dot{\mathbf{X}} = -\mathbf{M}\mathbf{X} \tag{1}$$

where the dot denotes the time derivative. The eigenvalues of **M** are the reciprocals of the relaxation times τ_i. Amplitudes A_i^0 corresponding to each τ_i are given by (Crothers, 1971b)

$$A_i^0 = \sum_k \Delta\epsilon_k T_{ki} \sum_j T_{ij}^{-1} X_j^0 \tag{2}$$

where T_{ki} is an element of the matrix which diagonalizes **M** by a similarity transformation, $\Delta\epsilon_k$ is the difference in extinction coefficients between species k and a designated reference species, and X_j^0 is the difference between the equilibrium concentrations of species j before and after the perturbation. X_j^0 is calculated from the T_m's and ΔH's for each reaction step. For the relaxation times the reverse rate constant of each reaction step is calculated from its value at T_m and its activation energy by the Arrhenius equation, and the forward rate constant is then calculated using the equilibrium constant which is determined by T_m and ΔH. Calculations were performed on an IBM 370 computer.

Figure 2 shows a computer simulation for the temperature dependence of the relaxation *amplitudes* for the simplest mechanism which can exhibit coupling:

$$A \overset{\text{slow}}{\rightleftharpoons} B \overset{\text{fast}}{\rightleftharpoons} C$$

T_{mBC} = 62°C, and T_{mAB} is varied while other parameters are held constant. In (a) T_{mAB} = 45°C, and the relaxations are effectively uncoupled. τ_s(slow) corresponds to the melting of A to B and τ_f(fast) to B melting to C. In (b) $T_{mAB} = T_{mBC}$ and weak coupling occurs; τ_s increases and narrows while τ_f decreases. Also, the amplitudes no longer peak exactly at T_m. In (c) T_{mAB} = 79°C, and τ_s has increased and narrowed greatly while τ_f has effectively disappeared. τ_s now corresponds effectively to A melting directly to C.

The similarity between the computer simulation and the data presented in Figure 1 is evident. It appears that τ_2, the slow tertiary-D helix melting is selectively stabilized by Mg^{2+} and couples into the microsecond relaxations, eventually causing the whole molecule to melt together as a single relaxation.

The basic mechanism we will use for interpreting the data for the major relaxation τ_2 is

$$N \underset{k_{23}}{\overset{k_{32}}{\rightleftharpoons}} T^-X^- \underset{k_{12}}{\overset{k_{21}}{\rightleftharpoons}} T^-X^-Y^- \rightarrow \left\{\begin{array}{l}\text{melting of remaining} \\ \text{structure at higher } T_m\end{array}\right\} \quad (3)$$

slow fast

where X and Y are unspecified regions of the molecule and T is the tertiary structure. In this mechanism T^-X^- is a transient intermediate only slightly populated, so that τ_2 refers essentially to melting of native structure N to the form $T^-X^-Y^-$ lacking interaction regions T, X, and Y. X and Y are introduced so that we can distinguish between the structure Y formed before the rate-limiting step in refolding, and the structure X which dissociates with the tertiary structure in the rate-limiting step of unfolding. Anticipating our results briefly, we will show that Y is probably always the D helix, and X increases as the Mg^{2+} concentration increases. Without Mg^{2+}, X = 0, but with high Mg^{2+} X consists of the TψC, anticodon, and acceptor stem helices. In this latter limit, the whole melting process is essentially a two-state, all-or-none conversion from native structure to random coil.

(*c*) *Relaxation Times.* The temperature dependences of τ_2 in the absence of Mg^{2+} and at 3.0 m*M* Mg^{2+} are shown in Figure 3. The increase in τ_2 with temperature on the low temperature side of the transition indicates that the process is not an elementary step, A ⇄ B, since the data imply a negative activation energy for forming the native structure.

It is common in considering the rates of nucleic acid structure formation to use information about activation energies to draw conclusions concerning the heat content of the nucleus required for the rate-limiting step (Pörschke and Eigen, 1971; Craig et al., 1971). Consider formation of the native structure N from the species $T^-X^-Y^-$ lacking the tertiary structure and other regions X and Y of the molecule, through the intermediate T^-X^-, as shown in eq 3. We call Y the nucleus required for formation of the tertiary structure. When $k_{21} \gg k_{23}$, T^-X^- is in steady-state preequilibrium with $T^-X^-Y^-$, and the forward rate constant for producing N is approximately $k_f = K_{12}k_{23}$. Similarly, the reverse constant is $k_r = k_{32}$. As is customary in such an analysis (Pörschke and Eigen, 1971; Craig et al., 1971) we assume that the elementary reaction rate for structure formation has negligible activation energy. Therefore the apparent (negative) activation energy for structure formation $E_f^\dagger$ is minus the enthalpy ΔH_Y of melting the nucleus. Similarly, the activation energy $E_r^\dagger$ for dissociation is the enthalpy of melting X and T, or ΔH_{X+T}.

Figure 3 shows theoretical curves for the relaxation time, calculated by the computer program described in the previous section, compared with the experimental results. We

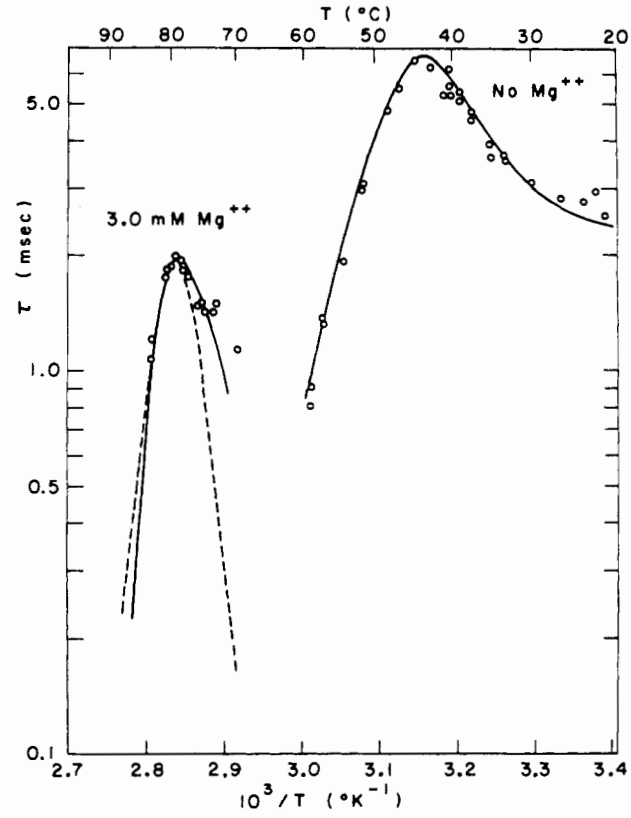

FIGURE 3: Comparison of experimental and calculated temperature dependence of the slow relaxation time τ_2 for no Mg^{2+} and 3 m*M* Mg^{2+}. For the fitted curve at no Mg^{2+} ΔH_X = 0, ΔH_T = 38, and ΔH_Y = 32 kcal/mol; the solid fitted curve at 3 m*M* Mg^{2+} corresponds to ΔH_{X+T} = 131 and ΔH_Y = 32 kcal/mol; the nonfitting dashed curve at 3m*M* Mg^{2+} represents ΔH_{X+T} = 80 and ΔH_Y = 86 kcal/mol (D and TψC arms as a nucleus for tertiary structure formation). Other parameters and details concerning the data fitting are given in Table II.

found that the data could be fitted with ΔH_Y = 32 kcal/mol at all Mg^{2+}, and with ΔH_{X+T} varying from 38 kcal/mol at low Mg^{2+} to 131 kcal/mol at high Mg^{2+}. (The sum $\Delta H_Y + \Delta H_{X+T}$ is the difference between forward and reverse activation energies and must, of course, equal the enthalpy of the whole melting transition, measured from the width of the differential melting curve.) Parameters used for the calculation are given in detail in Table II.

The conclusion from this analysis is that under all conditions a structure Y with 32 kcal/mol enthalpy of melting is required in order to nucleate the formation of tertiary structure. Furthermore, in the absence of Mg^{2+} the curvature of log τ_2 vs. $1/T$ below T_m allows estimation of the T_m for the region Y. The result is 35°C. Reasons for assigning the D helix as the nucleus Y are considered in the Discussion. The amount of structure X that melts with T in τ_2 increases with the Mg^{2+} concentration, as shown by the disappearance of the fast relaxations τ_3 and τ_4, and the concomitant increase in the enthalpy of τ_2.

(*d*) *Mg^{2+} Released upon Melting Known Regions of tRNA.* The coupling of melting transitions by preferential Mg^{2+} stabilization of the tertiary interactions indicates that at least to a first approximation, regions of the tRNA melt together increasingly as the Mg^{2+} concentration is raised, and that this melting is manifested in τ_2. The melting reaction τ_2 is approximated by

$$N \rightleftarrows T^-X^-Y^- \quad (4)$$

where at low Mg^{2+} concentrations X + Y is just the D arm

Table II: Thermodynamics and Kinetic Parameters for the Fitted Curves in Figure 3, Calculated as Described in the Text.[a]

$$\text{mechanism} = N \underset{k_{23}\ \text{slow}}{\overset{k_{32}}{\rightleftharpoons}} T^{-}X^{-} \underset{k_{12}\ \text{fast}}{\overset{k_{21}}{\rightleftharpoons}} T^{-}X^{-}Y^{-} \rightarrow \left\{\begin{matrix}\text{melting of remaining} \\ \text{structure at higher } T_m\end{matrix}\right\}$$

Structure Implied by X and Y; Mg^{2+} Concn	T_{mT+X} (°C)	ΔH_{T+X} (kcal/mol)	T_{mY} (°C)	ΔH_Y (kcal/mol)	k_{23} (sec^{-1})
A					
X: no structure	54.8	38	35.0	32	4.63×10^2
Y: D helix					
No Mg^{2+}					
B					
X: Anticodon helix and TψC helix	94.5	131	35.0	32	2.76×10^5
Y: D helix					
3 m*M* Mg^{2+}					
C					
X: Anticodon	115.5	80	50.8	86	1.15×10^7
Y: D helix and TψC helix					
3 m*M* Mg^{2+}					

[a] Activation energies for the structure formation rate constants k_{23} and k_{12} were assumed to be zero. k_{12}, the fast formation rate constant, was assigned a constant value of 5.0×10^4 sec^{-1}, a typical value for the formation rate constant of a hairpin helix ($\tau \approx 10$ μsec). In (A) all parameters were varied in order to obtain the best fit to the relaxation amplitude and relaxation time as a function of temperature. In (B) T_{mY} and ΔH_Y were assigned the values from fit (A) and T_{mT+X} and ΔH_{T+X} were varied to obtain the best fit to the relaxation data. In (C) an additional 54 kcal, corresponding to the *uncoupled* TψC helix melting at 61°C (Crothers et al., 1974) was added to ΔH_Y; T_{mY} is the temperature for which ΔG° for the complete transition $T^{-}X^{-} \rightarrow T^{-}X^{-}Y^{-}$ is zero. Case (C) is shown to indicate the lack of fit to a model with a larger nucleus Y.

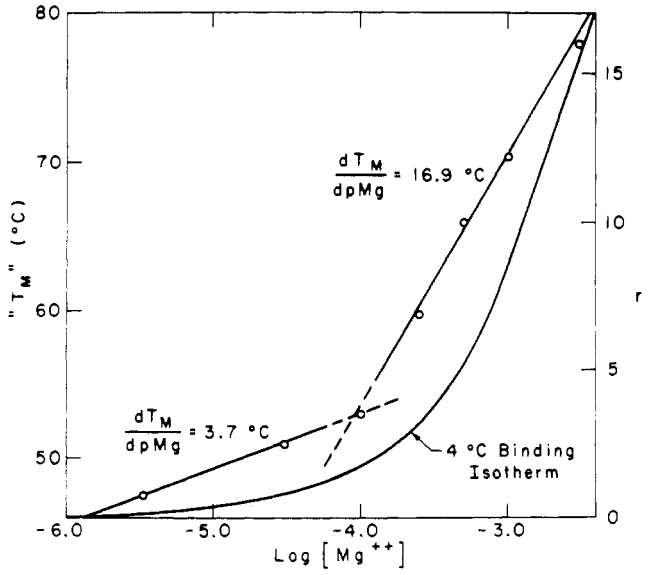

FIGURE 4: "T_m," the temperature of maximum amplitude for the slow relaxation τ_2 and the curve representing r, the number of Mg^{2+} ions bound/tRNA at 4°C (Stein and Crothers, 1976), vs. the logarithm of the Mg^{2+} concentration.

(X = 0), becoming at higher Mg^{2+} concentrations the D and TψC arms; at high Mg^{2+} the whole molecule melts together from native form to coil. This approximation allows the calculation of the number of Mg^{2+} ions released upon the melting of known parts of the tRNA.

For a helix–coil melting equilibrium coupled with a small molecule binding equilibrium the following relation holds (Crothers, 1971a):

$$\Delta r = (dT_m/\text{dpMg})[(\Delta H_a')_m/2.3RT_m^2] \qquad (5)$$

where Δr is the number of Mg^{2+} ions released upon melting, $(r_h - r_c)$, according to the stoichiometric equation

$$\text{helix}(r_h Mg^{2+}) \rightleftarrows \text{coil}(r_c Mg^{2+}) + (r_h - r_c)Mg^{2+}$$

at Mg^{2+} activity a. $(\Delta H_a')_m$ is the heat of melting at T_m and Mg^{2+} activity a and includes the extra heat of Mg^{2+} binding. The change in T_m with log [Mg^{2+}] is shown in Figure 4 along with the Mg^{2+} binding isotherm at 4°C. Pertinent data are given in Table I. The values of ΔH and Δr for the highest Mg^{2+} concentration are likely to be low due to the sharpness of the transition and possibly the incomplete melting of the acceptor stem.

(f) Direct Measurement of Mn^{2+} Released upon Tertiary Unfolding. At low "free" Mg^{2+} or Mn^{2+} concentrations ($\approx 1 \times 10^{-5}$ *M*) the melting of the tertiary–D helix interactions is well separated in temperature and time from the other transitions and may be treated independently to a good approximation. If Mn^{2+} is released during this unfolding, a decrease in fluorescence should be observed in the fluorescent temperature-jump experiment with the same characteristic 5-msec relaxation time as the absorbance signal due to the perturbation of the fast metal–dye equilibrium by the slowly relaxing melting equilibrium. Figure 5a shows the *absorbance* relaxation signal at 51°C, the T_m of the tertiary–D helix transition at 3.0×10^{-5} *M* Mg^{2+} (or Mn^{2+}), and Figure 5b shows the *fluorescence* signal at 50°C due to the release of Mn^{2+} at a "free" Mn^{2+} concentration of 1.4×10^{-5} *M*. The relaxation time is 5 msec and the amplitude reaches its maximum at 50°C, just where the tertiary–D helix T_m should be according to the Mg^{2+} data in Figure 4. The "free" Mn^{2+} concentration was calculated from the binding constant of the dye, the dye concentration, and total Mn^{2+} concentration. Taking into account the Mn^{2+} bound to tRNA (≈ 7 μ*M*) leads to a negligible correction.

From the amplitude of this relaxation signal the number of Mn^{2+} ions released upon the melting of the tertiary–D helix interactions can be calculated. The melting equilibrium is (X = 0, Y = D)

$$N(rMn^{2+}) \rightleftarrows T^{-}D^{-}(r'Mn^{2+}) + \Delta rMn^{2+}$$

because the Mn^{2+} concentration is low and earlier results (Crothers et al., 1974) show that the transition τ_2 consists

of melting the tertiary structure and D helix under these conditions. From the stoichiometry of the reaction:

$$\Delta r = (r - r') = \Delta C_{Mn^{2+}}/\Delta C_N \quad (6)$$

where $\Delta C_{Mn^{2+}}$ and ΔC_N denote the concentration changes of these species. Therefore,

$$\Delta r = (dF/dC_{Mn^{2+}})^{-1}(\Delta F/\Delta C_N) \quad (7)$$

where $dF/dC_{Mn^{2+}}$ is the fluorescence change per unit change in Mn^{2+} concentration under the conditions of the experiment and ΔF is the amplitude of the relaxation signal. $\Delta F/\Delta C_{Mn^{2+}}$ was determined to be 36 mV/μM, ΔF = 45 mV, and at T_m

$$\Delta C_N = \Delta H C_T \Delta T/4RT_m^2 \quad (8)$$

where ΔH = 61 kcal/mol, T_m = 50.0°C, the temperature-jump size ΔT = 2.71°C, and the total tRNA concentration $C_T = 2.0 \times 10^{-5}$ M. Using these values $\Delta r = 0.31 \pm 0.05$. From the Mg^{2+} binding data at 4°C (Stein and Crothers, 1976) the number of strongly bound metal ions at a free metal ion concentration of 1.4×10^{-5} M is 0.29 (0.15 weakly bound) corresponding closely to the number of Mn^{2+} ions released. This result, and those of the previous section show that unfolding the tertiary structure leads to loss of the strong binding site, with a rate of ion release equal to the rate of structural unfolding.

We stress that these results do *not* mean that the equilibrium between free and bound Mn^{2+} (or Mg^{2+}) attached to the native or unfolded forms occurs at the rate of unfolding the tertiary structure. Rather, since we see only a single relaxation time for ion release under conditions where individual tRNAs have different numbers of ions bound, the separate ion binding equilibria must be rapid:

$$M^{2+} + N \rightleftarrows N(r_1M^{2+}) \rightleftarrows T^-X^-(r_2M^{2+}) \rightleftarrows T^-X^- + M^{2+}$$

fast ion binding equilibrium — slow unfolding and coupled ion release — fast ion binding equilibrium

In this equilibrium, r_1 and r_2 ($r_1 > r_2$) are the average number of ions bound per mole of native (N) and unfolded (T^-X^-) tRNA. Since the enthalpy of ion binding is near zero, we could not measure signals due to the fast equilibria. The slow ion release we measure arises because native and unfolded forms differ strongly in affinity for divalent metal ions. The release of ions with relaxation time τ_2 shows clearly that *the structure responsible for strong ion binding unfolds in relaxation process* τ_2.

Discussion

(*a*) *Identification of Relaxation Signals.* We have assumed for analysis of the results reported here that the previously determined order of melting events in $tRNA^{fMet}$ is valid. Recently reported investigations raise legitimate questions in this regard. In particular, some of the resonance assignments used in our earlier study (Crothers et al., 1974) have become questionable because of the discovery of resonances associated with tertiary hydrogen bonds (Hilbers and Shulman, 1974; Wong and Kearns, 1974a; Daniel and Cohn, 1975). Of special interest for $tRNA^{fMet}_1$ is the careful study by Daniel and Cohn (1975), who showed that removal of the contaminating photocross-linked $tRNA^{fMet}_1$ produced an NMR spectrum with much-improved peak resolution. They estimated 27 ± 1 exchangeable protons in the region −11 to −15 ppm, compared to the assumed value of

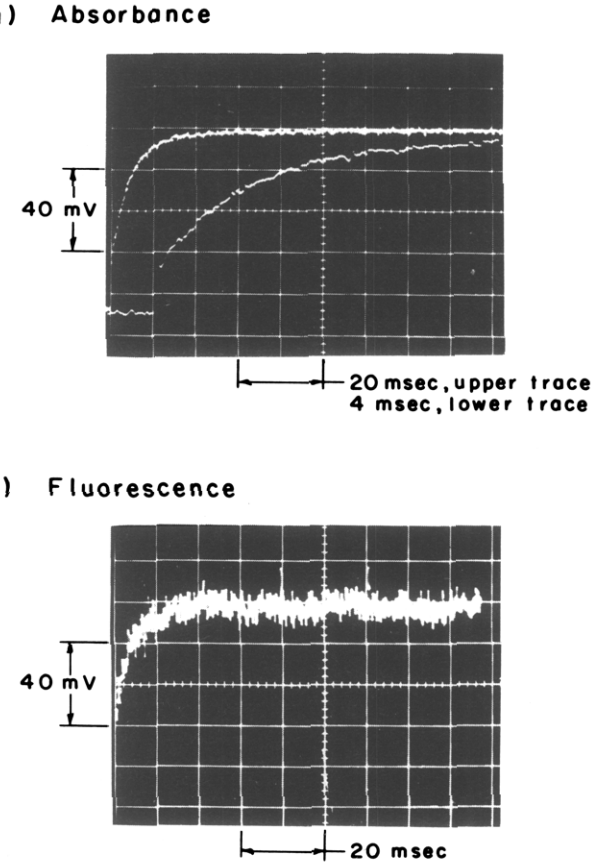

FIGURE 5: Oscilloscope traces of the 5-msec relaxation characteristic of the tertiary–D helix melting in the presence of low concentrations of Mg^{2+} or Mn^{2+}. (a) Absorbance signal, 266 nm at 51°C, 3.0×10^{-5} M Mg^{2+}, is due to tertiary–D helix melting; (b) fluorescence signal, excitation wavelength 368 nm, 50°C, 1.4×10^{-5} M Mn^{2+}, is due to Mn^{2+} ions released upon melting tertiary–D helix interactions.

19, equal to the number of cloverleaf base pairs, which we adopted in our earlier study (Crothers et al., 1974).

In reexamining our earlier data it is evident that the tertiary resonances do not appear as well-defined peaks in our thermal difference spectra, probably because of the partial photomodification of the structure. For example, the thermal difference spectrum we associated with melting of the anticodon helix contained a broad and barely detectable contribution from 14.3 to 14.8 ppm which we assigned to one proton in A·U base pair 28. The work of Daniel and Cohn (1975) indicates that the region probably contains two tertiary resonances; AU 28 is more likely to be found at 12.8 ppm (Wong and Kearns, 1974b). It is probable that there is some additional contribution by nonintegral tertiary resonances to the thermal difference spectrum we measured for melting the anticodon helix, especially since the T-jump measurements indicate that the tertiary structure is actually melting in the same temperature range.

In considering the problem of the order of melting of tRNA structure, it is worth recalling that the T-jump shows four relaxations for $tRNA^{fMet}_1$, and the NMR investigation is based on a data set of at least 19 resonances. It is evident that some error can be tolerated in the larger set without necessarily implying error in the assignment of the four relaxations. We do not see grounds for reversing any of our assignments of the order of optical melting of the various cloverleaf arms, especially since the assignment made is consistent with the predicted stability order of the helices (Crothers et al., 1974). The identification of the tertiary

melting relaxation is strongly supported by the influence of single base changes in regions not hydrogen bonded in the cloverleaf (Crothers et al., 1974; Leon, V., Altman, S., and Crothers, D. M., to be published), by earlier spectroscopic arguments (Cole et al., 1972), and by the finding reported in this paper that the structure that melts in the "tertiary" relaxation is responsible for the strong Mg^{2+} binding site. The D helix melting is included in the melting of tertiary structure because no separate relaxation signal was found for its melting, and because stability predictions indicated it should melt at the T_m of the tertiary structure. Simultaneous unfolding of the D helix and tertiary structure is entirely consistent with the close involvement of the D helix and tertiary structure revealed by x-ray diffraction studies (Robertus et al., 1974; Kim et al., 1974).

Finally, Wong et al. (1975) reported significantly different results on the melting of $tRNA^{fMet}$ measured by NMR than we found (Crothers et al., 1974). The simplest explanation is that their samples are not really Mg^{2+} free, so that the two measurements are not strictly comparable. In our early attempts at the problem we had difficulty removing Mg^{2+} from the concentrated tRNA samples prepared for NMR measurements. We were not satisfied on this point until the optically observed T_m for the tertiary melting transition, measured at 335 nm, was the same in high and low concentration tRNA samples. Comparable control measurements were not reported by Wong et al. (1975), and it is evident from their spectra that the tertiary melting transition occurs at higher temperature than we found. The results of our present paper show this to be the expected effect of small amounts of Mg^{2+}. In any event, T-jump measurements are much better suited for providing a simple picture of tRNA unfolding than are NMR measurements, which detect primarily transient opening of helices, not unfolding. Furthermore, the NMR approach seems to be subject to continuing uncertainty on resonance assignments.

(*b*) *Qualitative Effects of* Mg^{2+}. It is clear that at 0.17 *M* Na^+ ion concentration, Mg^{2+} preferentially stabilizes the tertiary and D helix interactions. Upon increasing the Mg^{2+} concentration to about 1×10^{-4} *M* the *sole* effect on the high resolution differential melting curve is a stabilization of the first peak corresponding to τ_2, the tertiary–D melting. As indicated in Table I, the T_m corresponding to τ_2 increases by about 8°C while the enthalpy remains about the same. τ_2 decreases slightly, but there is no significant change in the relaxation spectrum indicating that no rearrangement of base pairs or major reordering takes place when Mg^{2+} is added.

Upon addition of more Mg^{2+} the relaxation spectrum gradually changes as shown in Figure 1. If the melting of each part of the molecule were truly independent, τ_2 would be expected to shift to higher temperatures without affecting the other relaxation processes. The observed behavior indicates that other parts of the molecule cannot melt independently when the tertiary structure is intact. Similar qualitative observations on coupling effects due to Mg^{2+} have been reported (Riesner et al., 1970; Römer et al., 1970a,b). Changes in the relaxation spectrum are qualitatively those predicted from the simplest considerations of coupling, such as the simulated effect illustrated in Figure 2, and can be fitted in detail by the mechanism 3.

(*c*) *Nature of the Nucleus for Refolding.* According to eq 3 and the experimental data in Figure 3, the relaxation kinetics for τ_2 imply a nucleus Y for refolding the tertiary structure with an enthalpy of melting $\Delta H_Y = 32$ kcal/mol, independent of Mg^{2+} concentration. Several lines of evidence indicate that Y is the D helix. First, the known mechanism of melting without Mg^{2+} has only the D helix and tertiary (T) interaction melting in the first transition. In this case there is no plausible alternative for Y, unless we assume that Y is part of the tertiary structure itself. Second, the T_m (35°C) and enthalpy (32 kcal) found for Y (when T is melted; see Table II) are in reasonable agreement with predicted properties of the isolated D helix, based on parameters (Gralla and Crothers, 1973) that yield accurate values for other $tRNA^{fMet}$ helices (Crothers et al., 1974). The predicted T_m for the isolated D helix is 47°C, with predicted enthalpy 28 kcal/mol. The slightly lower measured T_m could be due to unusually large electrostatic interactions. Third, the crystal structure of $tRNA^{Phe}$ shows many bonds to the D helix, so it is structurally reasonable that the D helix be required in order to nucleate the tertiary bonding. Finally, recent results on $tRNA^{Gly}$ from wheat germ embryo (A. Stein, unpublished results) in which the D arm is extremely unstable, 1 A·U and 2 G·U base pairs (B. Roe, personal communication), show that the rate constant for tertiary folding is several orders of magnitude slower than in $tRNA^{fMet}$. This is consistent with the D arm acting as a nucleus, since the smaller value of K_{12} in mechanism 3 would yield a smaller $k_f = K_{12}k_{23}$. The finding of Coutts et al. (1974) that the D helix in $tRNA^{Asp}$ is stabilized in the intact molecule far above the T_m in fragments is consistent with the mechanism proposed here.

(*d*) *Divalent Ion Release upon Melting Known Regions of tRNA.* Location of the strong binding site can be inferred from the results on the Mg^{2+} and Mn^{2+} released upon melting known regions of tRNA. Table I shows that at 3×10^{-5} *M* Mg^{2+} where only the tertiary–D helix interactions "melt out" at 51°C the average number of Mg^{2+} ions released in the transition τ_2, 0.48, is in close agreement with the number of strongly bound Mg^{2+} ions at 4°C, 0.47. This result implies that the strong binding site is lost when the tertiary and D helix interactions are lost. The conclusion is reasonable if the temperature dependence of the Mg^{2+} binding to the "native" form of tRNA is not very large. Enthalpies calculated from the low-Mg^{2+} relaxation data indicate that the heat of Mg^{2+} binding is small. Also, Rialdi et al. (1972) found that the enthalpy of Mg^{2+} binding to yeast $tRNA^{Phe}$ is near zero at 25°C by mixing calorimetry. Finally, the Mg^{2+} binding constant for several polynucleotides, under conditions similar to those reported here, is nearly temperature independent (Krakauer, 1971).

The data indicate that several Mg^{2+} ions are released upon the melting of the helical arms of tRNA indicating that these sections are stabilized to some extent by Mg^{2+}. The result that not all of the weakly bound Mg^{2+} ions are released upon melting indicates that the unfolded and possibly the single-stranded regions of tRNA still have an appreciable affinity for Mg^{2+}. Schreier and Schimmel (1974) assigned a class of about 12 Mn^{2+} sites to the cloverleaf helical sections of yeast $tRNA^{Phe}$ from binding studies with synthetic polynucleotides. They also found that single-stranded polynucleotides have an affinity for Mn^{2+} which depends significantly upon the base composition.

The fluorescence temperature-jump experiment shows directly that divalent ions are released upon melting of the tertiary and D helix interactions. The characteristic 5-msec relaxation signal reaching a maximum amplitude at 50°C identifies the transient increase in Mn^{2+} as arising from the tertiary–D helix melting. Calculation of the average num-

ber of Mn^{2+} ions released by a method independent of the other relaxation data again indicates that the number of Mn^{2+} ions released corresponds to the number of strongly bound Mg^{2+} ions at 4°C. Therefore, the single strong binding site on $tRNA^{fMet}_1$ must be assigned to a region of the molecule involved in maintaining tertiary interactions, most likely near the D arm.

(*e*) *Comparison with Earlier Work on $tRNA^{fMet}$.* Since this is the final paper in our present series on $tRNA^{fMet}$, we would like to clarify those points on which our present understanding has required revision of the interpretation of previous experiments. The most important matter concerns the difference in stability between $tRNA^{fMet}_1$ and $tRNA^{fMet}_3$. In our first paper on $tRNA^{fMet}$ relaxation kinetics (Cole and Crothers, 1972) we did not realize that $tRNA^{fMet}_3$ was an important contaminant in the sample of $tRNA^{fMet}_1$, which is supposedly the major species. We found two tertiary structure relaxations and concluded that the tertiary structure melts in two steps. This is incorrect. As we later reported (Crothers et al., 1974), the first relaxation (τ_1) refers to $tRNA^{fMet}_3$ and the second (τ_2) to $tRNA^{fMet}_1$. Melting of tertiary structure in $tRNA^{fMet}_1$ shows only one relaxation, demonstrated clearly by the present results. Furthermore, since it was not necessary to resolve τ_1 and τ_2 in the experiments reported here, the temperature dependence of τ_2 could be determined much more accurately than previously. This accounts for our earlier failure to detect the small negative activation energy of τ_2 below the T_m.

Finally, there is one point where the conflict with previous results is only apparent. Our earlier NMR studies (Crothers et al., 1974) indicated that the protons H-bonded in the D helix could exchange with solvent H_2O more rapidly than the tertiary structure could open. Yet in the present paper we interpret the results to mean that the D helix is a required nucleus for the tertiary structure. These results are mutually consistent if different paths dominate the kinetics of exchange and melting. For example, consider the mechanism:

$$\begin{array}{ccccc} N & \rightleftharpoons & T^- & \rightleftharpoons & T^-D^- \\ \uparrow\downarrow & & \text{melting} & & \\ & & \text{"breathing"} & & \\ T'D^- & & & & \\ \downarrow & & & & \\ \text{exchange} & & & & \end{array}$$

where the symbol $T'D^-$ represents a structural fluctuation or "breathing" mode in which the tertiary structure is altered sufficiently to allow the D helix to open transiently and undergo proton exchange. When the melting and exchange paths are separate, there is no necessary relation between their kinetics.

(*f*) *Functional Aspects of Folding.* Our results raise two significant points concerning the possible role of tRNA folding and unfolding in vivo. First, the tertiary structural stability of tRNA is very sensitive to Mg^{2+}. It is therefore plausible that selective ribosome-mediated removal of Mg^{2+} from tRNA could trigger unfolding of the native structure. Bonds between tRNA and rRNA might also stabilize the unfolded structure. Refolding induced by return of Mg^{2+} at some later stage would result in a cyclic tRNA conformational change with important consequences for the mechanics of protein synthesis.

Second, our results are indirectly relevant to the problem of folding tRNA or its precursor during biosynthesis. It appears that nucleation of the tertiary structure requires just the D helix and at least some of the bases involved in tertiary bonding. The intact TψC helix is not required, for example. This means that the tertiary structure can be formed before biosynthesis is complete, which may be one of the ways incorrect conformational structures are avoided.

References

Bina-Stein, M., and Crothers, D. M. (1975), *Biochemistry 14,* 4185.

Cole, P. E. (1972), Ph.D. Thesis, Yale University.

Cole, P. E., and Crothers, D. M. (1972), *Biochemistry 11,* 4368-4374.

Cole, P. E., Yang, S. K., and Crothers, D. M. (1972), *Biochemistry 11,* 4358-4368.

Coutts, S. M., Gangloff, J., and Dirheimer, G. (1974), *Biochemistry 13,* 3938-3948.

Craig, M. E., Crothers, D. M., and Doty, P. (1971), *J. Mol. Biol. 62,* 383-401.

Crothers, D. M. (1971a), *Biopolymers 10,* 2147-2160.

Crothers, S. M. (1971b), *Proced. Nuclic Acid Res. 2,* 369.

Crothers, D. M. (1975), in Functional Linkage in Biomolecular Systems, Schmitt, R. O., Schnieder, D. M., and Crothers, D. M., Ed., New York, N.Y., Raven Press, pp 30-32.

Crothers, D. M., Cole, P. E., Hilbers, C. W., and Shulman, R. G. (1974), *J. Mol. Biol. 87,* 63-88.

Daniel, W. E., and Cohn, M. (1975), *Proc. Natl. Acad. Sci. U.S.A. 72,* 2582-2586.

Diehl, H. (1964), Calcein, Calmagite and *O,O'*-Dihydroyazobenzene. Titrimetric, Calorimetric and Fluorometric Reagents for Calcium and Magnesium, Columbus, Ohio, The G. Frederick Smith Chemical Company, p 87.

Erdman, V. A., Sprinzel, M., and Pongs, O. (1973), *Biochem. Biophys. Res. Commun. 54,* 942-948.

Gralla, J., and Crothers, D. M. (1973), *J. Mol. Biol. 73,* 497.

Hilbers, C. W., and Shulman, R. G. (1974), *Proc. Natl. Acad. Sci. U.S.A. 71,* 3239-3242.

Kim, S. H., Sussman, J. L., Suddath, F. L., Quigley, G. J., McPhersen, A., Wang, A. H. J., Seeman, N. C., and Rich, A. (1974), *Proc. Natl. Acad. Sci. U.S.A. 71,* 4970-4974.

Krakauer, H. (1971), *Biopolymers 10,* 2459-2490.

Pörschke, D., and Eigen, M. (1971), *J. Mol. Biol. 62,* 361-381.

Rialdi, G., Levy, J., and Biltonen, R. (1972), *Biochemistry 11,* 2472-2482.

Riesner, D., Römer, R., and Maass, G. (1970), *Eur. J. Biochem. 15,* 85-91.

Robertus, J. D., Ladner, J. E., Finch, J. T., Rodes, D., Brown, R. S., Clark, F. F. C., and Klug, A. (1974), *Nature (London) 250,* 546-551.

Römer, R., Riesner, D., Coutts, S. M., and Maass, G. (1970b), *Eur. J. Biochem. 15,* 77-84.

Römer, R., Riesner, D., and Maass, G. (1970a), *FEBS Lett. 10,* 352-357.

Schreier, A. A., and Schimmel, P. R. (1974), *J. Mol. Biol. 86,* 601-620.

Schwarz, U., Luhrmann, R., and Gassen, H. G. (1974), *Biochem. Biophys. Res. Commun. 56,* 807-814.

Stein, A., and Crothers, D. M. (1976), *Biochemistry,* preceding paper in this issue.

Wong, K. L., and Kearns, D. R. (1974a), *Nature (London) 252,* 738-739.

Wong, K. L., and Kearns, D. R. (1974b), *Biopolymers 13*, 371-380.
Wong, K. L., Wong, Y. P., and Kearns, D. R. (1975), *Biopolymers 14*, 749-762.
Yarus, M., and Rashbaum, S. (1972), *Biochemistry 11*, 2043-2049.

Preparation and Properties of the Repeating Sequence Polymers $d(A\text{-}I\text{-}C)_n \cdot d(I\text{-}C\text{-}T)_n$ and $d(A\text{-}G\text{-}C)_n \cdot d(G\text{-}C\text{-}T)_n$†

Robert L. Ratliff,* Donald E. Hoard, F. Newton Hayes, David A. Smith, and Donald M. Gray

ABSTRACT: The repeating sequence polymer $d(A\text{-}I\text{-}C)_n \cdot d(I\text{-}C\text{-}T)_n$ has been prepared using the chemically synthesized oligomers $d(A\text{-}G\text{-}C)_4$ and $d(C\text{-}T\text{-}G)_4$ and the DNA polymerase from *Micrococcus luteus*. The enzymatically synthesized polymer was used as template for preparation of $d(A\text{-}G\text{-}C)_n \cdot d(G\text{-}C\text{-}T)_n$. Both deoxyribonucleotide polymers were characterized by nearest neighbor analyses, buoyant density measurements in cesium chloride and cesium sulfate, melting temperature, and circular dichroism (CD) spectra. The ribopolymers $r(A\text{-}I\text{-}C)_n \cdot r(I\text{-}C\text{-}U)_n$ and $r(A\text{-}G\text{-}C)_n \cdot r(G\text{-}C\text{-}U)_n$ were transcribed from $d(A\text{-}I\text{-}C)_n \cdot d(I\text{-}C\text{-}T)_n$, and their CD spectra were compared with those of the respective deoxyribonucleotide polymers.

Model DNAs and RNAs have played important roles in the development of our present understanding of nucleic acid structure, function, and enzymology. Snythetic DNAs with repeating nucleotide sequences have been instrumental in elucidation of the genetic code (Khorana et al., 1966) and in determination of repressor binding properties (Riggs et al., 1972). Synthetic DNA properties, such as buoyant density, have been used to derive relationships that describe the corresponding properties of natural DNA (Gray et al., 1974). Another type of model DNA has been used to study the influence of nucleotide composition in one region of a duplex DNA on the properties of a remote but contiguous region (Burd et al., 1975). It is clear from all these studies that the properties of a DNA depend upon its nucleotide sequence. For a recent review of the influence of nucleotide sequence on DNA properties, see Wells and Wartell (1974). Here we report the synthesis of both the new repeating trinucleotide DNA $d(A\text{-}G\text{-}C)_n \cdot d(G\text{-}C\text{-}T)_n$[1] and its analogue $d(A\text{-}I\text{-}C)_n \cdot d(I\text{-}C\text{-}T)_n$. Both polymers have been characterized by nearest neighbor analysis, buoyant density in cesium chloride and cesium sulfate, melting temperature, circular dichroism (CD) spectra, and ability to serve as template for RNA polymerase. A preliminary report of some of this work has been presented previously (Ratliff et al., 1974).

Experimental Procedures

Chemicals and Reagents. Unlabeled deoxyribonucleoside mono- and triphosphates, ITP, and ^{14}C-labeled ribonucleoside triphosphates were obtained from Schwarz/Mann and unlabeled ribonucleoside triphosphates from P-L Biochemicals. The α-^{32}P labeled deoxyribonucleoside and ribonucleoside triphosphates came from New England Nuclear. The dITP and [α-^{32}P]dITP were prepared by nitrous acid deamination of dATP and [α-^{32}P]dATP, respectively (Inman and Baldwin, 1964). 2-Mesitylenesulfonyl chloride, 2,4,6-triisopropylbenzenesulfonyl chloride, and *N,N'*-dicyclohexylcarbodiimide were purchased from Aldrich Chemical Co. The sulfonyl chloride reagents were recrystallized from petroleum ether immediately before use. Hydracrylonitrile (Eastman) was fractionally distilled under vacuum. Pyridine used as solvent in the chemical syntheses was distilled successively from chlorosulfonic acid and solid potassium hydroxide, then dried over a molecular sieve (Linde, type 3A). Cesium chloride and cesium sulfate were obtained from Harshaw Chemical Co. Agarose for gel permeation chromatography (Bio-Rad Laboratories) was purchased from Calbiochem. Whatman DE32 cellulose was employed for ion-exchange chromatography of chemically synthesized oligonucleotides.

Enzymes. Micrococcal DNase and alkaline phosphatase were purchased from Worthington Biochemical Corp. Snake venom phosphodiesterase was obtained from Calbiochem. Spleen phsophodiesterase was prepared by the methods of Hilmoe (1960) and Richardson and Kornberg (1964). *Micrococcus luteus* DNA polymerase, prepared ac-

† From the Cellular and Molecular Biology Group, Los Alamos Scientific Laboratory, University of California, Los Alamos, New Mexico 87545 (R.L.R., D.E.H., F.N.H., and D.A.S.), and the Institute for Molecular Biology, University of Texas at Dallas, Richardson, Texas 75080 (D.M.G.). *Received June 10, 1975.* That portion of the work conducted at the Los Alamos Scientific Laboratory was performed under the auspices of the U.S. Energy Research and Development Administration. Work at the University of Texas at Dallas was supported by Public Health Service Research Grant No. GM 19060 from the National Institute of General Medical Sciences and Grant No. AT-503 from the Robert A. Welch Foundation.

* Address correspondence to this author at the Los Alamos Scientific Laboratory, University of California, (MS-886), Los Alamos, New Mexico 87545.

[1] The abbreviation notation for complementary double-stranded polydeoxyribotrinucleotides is in one of the two general forms recommended by the IUPAC-IUB Combined Commission on Biochemical Nomenclature (1970) and further incorporates an alphabetization convention that allows only one way to write the structure of each polymer. The left-hand member of the notation is stated as the alphabetically earliest three-letter set of the six possibilities in the polymer. The right-hand member is then fixed to be complementary in reverse order of letters.